TISSUE ENGINEERING: Part C
Volume 29, Number 7, 2023

DOI: 10.1089/ten.tec.2023.0082

termis
Tissue Engineering
& Regenerative Medicine
International Society

Open camera or QR reader and scan code to access this article and other resources online.

REVIEW ARTICLE

Three-Dimensional Printing Bioceramic Scaffolds Using Direct-Ink-Writing for Craniomaxillofacial Bone Regeneration

Vasudev Vivekanand Nayak, MSci, PhD,[1] Blaire V. Slavin, BS,[2] Edmara T.P. Bergamo, DDS, PhD,[3,4] Andrea Torroni, MD, PhD,[5] Christopher M. Runyan, MD, PhD,[6] Roberto L. Flores, MD,[5] F. Kurtis Kasper, PhD,[7] Simon Young, DDS, MD, PhD,[8] Paulo G. Coelho, MD, DDS, PhD, MBA,[1,9] and Lukasz Witek, MSci, PhD[3,5,10]

Defects characterized as large osseous voids in bone, in certain circumstances, are difficult to treat, requiring extensive treatments which lead to an increased financial burden, pain, and prolonged hospital stays. Grafts exist to aid in bone tissue regeneration (BTR), among which ceramic-based grafts have become increasingly popular due to their biocompatibility and resorbability. BTR using bioceramic materials such as β-tricalcium phosphate has seen tremendous progress and has been extensively used in the fabrication of biomimetic scaffolds through the three-dimensional printing (3DP) workflow. 3DP has hence revolutionized BTR by offering unparalleled potential for the creation of complex, patient, and anatomic location-specific structures. More importantly, it has enabled the production of biomimetic scaffolds with porous structures that mimic the natural extracellular matrix while allowing for cell growth—a critical factor in determining the overall success of the BTR modality. While the concept of 3DP bioceramic bone tissue scaffolds for human applications is nascent, numerous studies have highlighted its potential in restoring both form and function of critically sized defects in a wide variety of translational models. In this review, we summarize these recent advancements and present a review of the engineering principles and methodologies that are vital for using 3DP technology for craniomaxillofacial reconstructive applications. Moreover, we highlight future advances in the field of dynamic 3D printed constructs via shape-memory effect, and comment on pharmacological manipulation and bioactive molecules required to treat a wider range of boney defects.

Keywords: 3D printing, scaffold, bone regeneration, *in vivo*, preclinical, regenerative medicine

[1]Department of Biochemistry and Molecular Biology, University of Miami Miller School of Medicine, Miami, Florida, USA.
[2]University of Miami Miller School of Medicine, Miami, Florida, USA.
[3]Biomaterials Division, New York University College of Dentistry, New York, New York, USA.
[4]Department of Prosthodontics and Periodontology, Bauru School of Dentistry, University of São Paulo, Bauru, São Paulo, Brazil.
[5]Hansjörg Wyss Department of Plastic Surgery, NYU Grossman School of Medicine, New York University, New York, New York, USA.
[6]Department of Plastic and Reconstructive Surgery, Wake Forest School of Medicine, Winston-Salem, North Carolina, USA.
[7]Department of Orthodontics, School of Dentistry, The University of Texas Health Science Center at Houston, Houston, Texas, USA.
[8]Bernard and Gloria Pepper Katz Department of Oral and Maxillofacial Surgery, School of Dentistry, The University of Texas Health Science Center at Houston, Houston, Texas, USA.
[9]DeWitt Daughtry Family Department of Surgery, Division of Plastic Surgery, University of Miami Miller School of Medicine, Miami, Florida, USA.
[10]Department of Biomedical Engineering, Tandon School of Engineering, New York University, Brooklyn, New York, USA.

Impact Statement

The development of three-dimensional printing (3DP) biomimetic, bioceramic scaffolds represents a significant breakthrough in the field of bone tissue regeneration (BTR). Combining the precision and flexibility of 3DP with the biocompatibility and resorbability of bioceramics has the potential to revolutionize the treatment of large boney defects. It also has the potential to address the shortage of autografts or reduce the risk of rejection or infection associated with allografts or xenografts. This technology can improve the quality of life for millions of people worldwide by providing an effective, safe, sustainable, and low-cost solution for BTR.

Introduction

THE HUMAN MUSCULOSKELETAL system is a contiguous structure that comprises of complex arrays of interconnected tissues.[1,2] While minor hard tissue injuries may heal with minimal to no surgical interventions, more complex cases associated with extensive trauma, oncologic resection, chronic osteomyelitis, or congenital defects often necessitate surgery.[3] The propensity toward these treatment modalities stems from the inadequacy of innate mechanisms of fracture or defect healing. Such scenarios may result in large, morphologically complex defects that will not heal through endogenous healing pathways thus requiring the use of natural or synthetic bone grafts.[3]

Bone grafting is one of the most commonly performed procedures worldwide, with a 2022 study reporting that over 4 million bone graft procedures were being performed in the United States annually and the bone graft substitutes market is valued at USD $3.78 billion.[4] According to a recent projection, the market has been predicted to grow to approximately USD $6 billion by 2029, driving research and development in the field.

Natural or synthetic bone grafts aid in hard tissue regeneration, facilitating the process to reestablish both form and function over time.[5] While autografting to date is considered the standard of care, ''gold standard'' for bone tissue regeneration (BTR) procedures, it is associated with a variety of drawbacks such as limited availability, pain, and donor site morbidity.[6–8] These shortcomings have propelled the development of alternatives, including synthetically derived grafts (alloplasts). Alloplasts have been extensively studied in BTR to effectively replicate/mimic the mechanical properties, bioactivity, and morphology, of native bone.[9,10] Of the different classes of alloplastic materials, ceramic-based materials have gained significant prominence as they provide a physiological environment that supports osteogenesis.[11–19]

Ceramics are synthesized solid, inorganic materials that are crystalline in nature. Bioceramics form a subset of this class, and are biocompatible, bioinert, bioactive, or bioresorbable. In particular, calcium phosphate ($CaPO_4$) CaP-based bioceramics have garnered increased attention as they can be utilized as resorbable, implantable devices.[11,14–16,18,19]

Grafts using CaP-based ceramics have traditionally been fabricated through the process of molding or casting. While the accuracy and precision of devices generated through these techniques are high, the process of mold preparation and refinement is laborious, especially for every patient or anatomic location that requires a customized, fit-and-fill graft. Furthermore, it is difficult to cast a part with controlled pore spacing and pore distribution—essential for biomimetic scaffold applications.[3] As such, over the course of time, surgeons have witnessed tremendous clinical and scientific innovations associated with craniomaxillofacial and orthopedic surgeries. This progress is attributed to the introduction of new techniques such as additive manufacturing, also commonly referred to as three-dimensional printing (3DP).[20–23]

Through 3DP of bioceramics, clinicians and engineers have been able to design and fabricate customized patient-specific implants or grafts, enabling restoration of form and function while maintaining physiological and aesthetic needs of patients.[24–27] Furthermore, 3D printing of resorbable bioceramics has enabled a reduction in time for bench-to-bedside translation, and a decrease in the need for secondary surgeries for hardware removal.[28]

The Need for Engineered Pore Architectures in Biomimetic Scaffold Design

Bone healing in the case of critically sized defects are either associated with lack of sufficient replacement of damaged tissue or presence of a fibrous network which compromises the reestablishment of form and function.[29–31] Subsequently, absence of vascularization and decreased stability of the residual bone can permanently hinder the healing process.[32,33] Such circumstances necessitate regenerative therapies to focus on the utilization of vascularized bone grafts.[34] As such, scaffold macrogeometry should permit adequate vascular supply that facilitates the delivery of oxygen, nutrients, and osteogenic progenitor cells.[35] Furthermore, scaffolds used in the restoration of bone defects in load bearing sites such as the mandible should exhibit sufficient mechanical strength.[36] Most importantly, ideal bone graft substitutes in craniomaxillofacial or orthopedic reconstructions are required to maintain symmetry and aesthetics while healing progresses.[3,37–40]

3DP technology has hence played a pivotal role in regenerative medicine by paving the way to customized soft and hard tissue reconstruction. It has allowed for the fabrication of patient-specific, space-maintaining scaffolds that are tailored to anatomic location-specific requirements.[41] Compared to conventionally used particulate bone grafts, 3D printed lattice-like scaffolds have been reported to mimic the external and internal architecture at the host site while also providing a template for cell attachment and migration.[3,38,42,43] 3D printed scaffolds have also been reported to provide improved structural stability helping reestablish the required tissue architecture.[3,38,42,43]

While an ideal scaffold presents excellent biocompatibility and the ability to support bone formation, sufficient mechanical strength and adequate pore size also allow for tissue growth and bone remodeling over the course of the rehabilitation.[37,44] When compared to granular or bulk constructs (devoid of engineered pores), the architecture

of 3D printed lattice-like structures has demonstrated improved biodegradability kinetics and osteoconductivity.[45,46]

Material Selection and Colloidal Gel Synthesis

Selection of a particular material for BTR necessitates a careful evaluation of material properties for successful preclinical or clinical translation (summarized in Table 1). Among the variety of different CaP ceramics available, β-tricalcium phosphate (β-TCP) [$Ca_3(PO_4)_2$] and Hydroxyapatite (HA) [$Ca_{10}(PO_4)_6(OH)_2$] are most commonly utilized in BTR.[47] HA is highly stable from a chemical standpoint and does not readily dissolve in biological fluids.[48] While this stability is essential for maintaining structural integrity, it leads to unfavorable resorption kinetics (~1% per year), which may increase risk of infection.[44,49] On the contrary, β-TCP is completely resorbable within a period between 6 and 18 months depending on the geometric configurations of the graft.[45] β-TCP has the added benefit of time-dependent kinematic surface modification capabilities. To elaborate, biologically active apatite layers form on the surface of β-TCP when exposed to ions found in blood plasma, thereby enhancing its bonding interface with the surrounding tissue.[50,51]

More importantly, due to the similarity in chemical composition of β-TCP to that of native bone, 3D printing technology has facilitated the fabrication of biomimetic bone scaffolds.[55] Of the various 3D printing platforms, solid

Table 1. Summary of Material Requirements for Ceramic Scaffolds Used in Bone Tissue Regeneration

Property	*Material requirement for ceramic scaffold use in BTR*	*Advantage of calcium phosphate-based ceramics*	*References*
Mechanical competence	Scaffolds aimed at regenerating bone defects should present the ability to withstand physiological loading or the ability to maintain shape during bone healing and remodeling processes. Immediate mechanical failure upon implantation could hamper healing and compromise aesthetics.	CaP scaffolds are not capable of load bearing *in vivo* without additional hardware—due to their brittle nature and low tensile strength. However, through subsequent osteoconduction and osseointegration with surrounding hard tissue, its mechanical strength has been reported to mimic that of cancellous bone.[29]	52,53
Chemical composition and resorbability	Ceramics for BTR must mimic the composition of native bone to hasten the bone healing process. Ideally, scaffolds should resorb over time (to avoid necessity of secondary hardware removal surgeries) at a rate that closely matches the rate of new bone formation.	The ratio of calcium to phosphorus in CaP-based ceramics, more specifically β-TCP, is close to that of natural bone tissue (~1.5). Furthermore, studies have reported favorable resorption rates of CaP scaffolds *in vivo* (rates dependent on ceramic composition, macro- and microgeometry of the scaffold).	45,54,55
Biocompatibility and bioactivity	Materials used in BTR must not only be biocompatible but also capable of promoting a favorable osteogenic response after scaffold insertion. The material used should boost bone healing either through intrinsic mechanisms or allow for augmentation with ionic components, or growth factors.	CaP bioceramics have been shown to exhibit exceptional biocompatibility and bioactivity. Studies have indicated that the application of β-TCP scaffolds alone can significantly increase bone regeneration relative to porous metal scaffolds.	56–59
Method of fabrication	Fabrication of a biomimetic scaffold must be cost-effective, commercially viable, and demonstrate reproducibility and repeatability. The method of fabrication should be capable of generating complex and intricate geometries to allow for rapid synthesis of patient/defect specific scaffolds. Furthermore, manufacturing methodology should allow for incorporation of interconnected pores and engineered pore architectures to facilitate nutrient flow while simultaneously permitting diffusion of waste and degradation products.	CaP-based colloidal gels have been reported to exhibit shear thinning and shape retention capabilities upon extrusion through DIW 3D printing (a form of rapid prototyping) to generate high fidelity scaffolds to treat critically sized boney defects. CaP-based colloidal gels and its integration with the DIW workflow has been shown to be a viable option in the fabrication of spanning structures and lattices with varied pore sizes (as low as ~100 μm) based on the shape and size of the defect requiring repair.	3,39,55,60

β-TCP, β-tricalcium phosphate; BTR, bone tissue regeneration; DIW, direct inkjet writing.

freeform fabrication or direct inkjet writing (DIW) has enabled the extrusion of high ceramic loaded colloidal gels due to ease of use and minimal postprocessing requirements.[10,39,43,55] DIW has allowed for 3DP of periodic structures with spanning features using colloidal gels with well-controlled viscoelastic responses and high-volume solid fractions.[61] A recent study highlighted the use of commercially available β-TCP along with other polymeric additives, namely, flocculants (polyethyleneimine), dispersants (ammonium polyacrylate), and viscosifiers (hydroxypropylmethylcellulose) to synthesize a colloidal gel capable of shear thinning and shape retention upon extrusion through a nozzle.[45,54]

Design of Biomimetic Scaffolds

Resorbable, biomimetic 3D printed scaffolds are typically engineered to be replaced with fully functional tissue during the final stages of healing to avoid the need for secondary hardware removal surgery.[37,44] In addition, engineered pore architectures aid in enhancing the overall mechanical strength of the construct in comparison to randomly distributed osteogenic particulate grafts.[62] It has been found that among the various methods by which scaffold resorption can be altered, manipulating scaffold architecture from the macroscale level can maximize a scaffold's capacity of driving bone formation in tandem with resorption kinetics.[37,44,45,63]

Advances in computer-aided design (CAD) (Fig. 1a) and its synergistic integration with microcomputed tomography (microCT) (Fig. 1b) have allowed for the reconstruction of the regions of interest (ROI). microCT imaging facilitates the capture of high-resolution image stacks of the ROI that can be digitally reconstructed using image thresholding and segmentation. In subsequent design steps, scaffold macrogeometric parameters are defined to adequately stabilize the defect site (Fig. 1c, d), with pore geometry sufficiently robust to impart the required mechanical integrity.[37,42,44] Subsequently, the reconstruction methodology involves the conversion of the segmented ROI to stereolithography (.stl) format through discretization—which helps produce high-fidelity defect templates that define the macrogeometry with a mesh of vertices and edge-sharing triangular facets.[64–66]

Once scaffold's macrogeometric parameters are determined, objects can be sliced using an appropriate slicing software to generate a multilayered three-dimensional (3D) object that comprised a series of parallel planes with fixed interplanar spacing. This slicing process converts the *.stl* into machine-level *.gcode*, which contains all the vital coordinate-related instructions along with auxiliary commands. These commands are especially useful in tailoring the scaffold lattice parameters, namely pore spacing, layer height, and rod size. Furthermore, the *.gcode* details the orientation of the scaffold to be printed, provides virtual builds of the scaffold for easy viewing, and allows print time optimization for rapid prototyping.

Printing and Postprocessing of Biomimetic Ceramic Scaffolds Using DIW

Three-axis motion on a DIW printer can be achieved by the tool path (.gcode) input to a computer numerical controller. DIW printers consist of a stationary platform equipped with a moveable gantry (Fig. 2a). The controller not only allows for gantry motion but also facilitates the plunger motion of syringe pumps loaded with the colloidal gels. Multiple extrusion nozzles allow the deposition of different colloidal gels simultaneously (Fig. 2b). More specifically, the primary printing material (such as β-TCP),

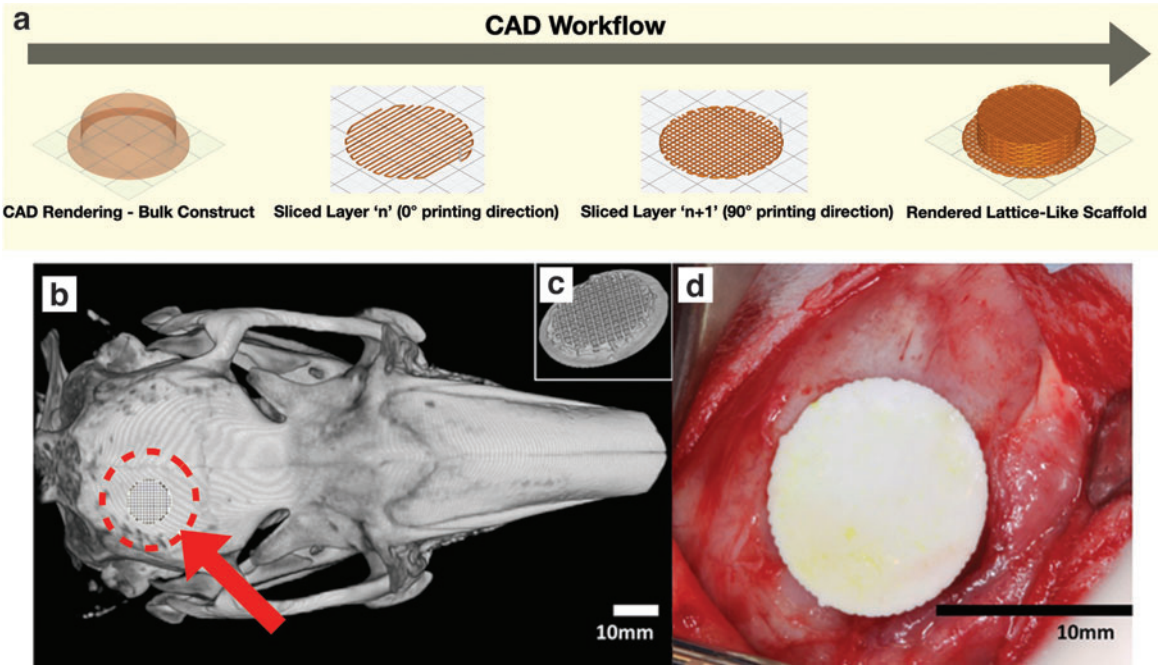

FIG. 1. **(a)** Biomimetic scaffold design CAD workflow schematic detailing layer-by-layer scaffold slicing and rendering (image not to scale), **(b)** schematic of location of unilateral calvarial defect (*dashed red circle* highlighting the region of interest), **(c)** inferior view of 3D diagram of printed calvarial scaffold, and **(d)** intraoperative image of fit-and-fill reconstruction of calvarial defect with scaffold.[45] CAD, computer-aided design.

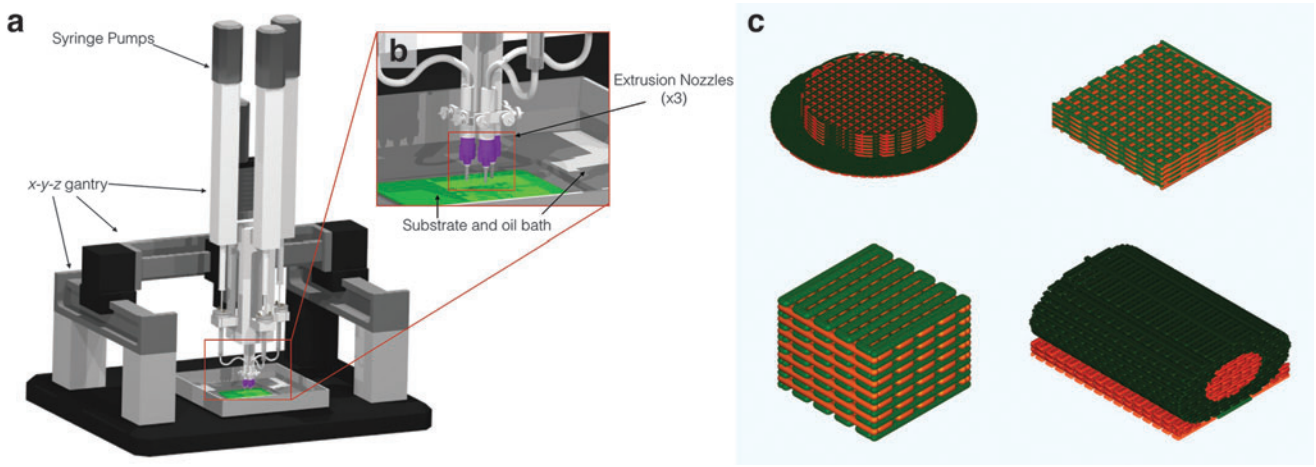

FIG. 2. **(a)** Schematic of robocasting machine (3D Inks LLC, Tulsa, OK) used to assemble bioceramic scaffolds, **(b)** magnified set-up of extrusion nozzles (3×) capable of codepositing multiple materials, **(c)** schematic of various scaffold macrogeometries capable of being extruded through DIW 3D printing of shear thinning bioceramic colloidal gels (images not to scale).[3] DIW, direct inkjet writing.

and fugitive support material (such as Carbon Black)—which is typically added during printing and then removed by dissolution or melting after the printing process is complete.

The use of fugitive support material allows for the creation of parts with internal cavities or overhangs that would be impossible to print without support (Fig. 2c). The extruders of the DIW printer follow the Cartesian coordinate tool path from the *.gcode* file while depositing the gel or slurry onto a substrate. Build times for the periodic structures (lattices or scaffolds) depend on a variety of factors ranging from overall scaffold volume, nozzle diameter (Fig. 3a–c), extrusion rate from the nozzle, and print velocity.

Printing of β-TCP colloidal gels is usually followed by sintering at high temperatures (Fig. 3d) increasing the overall mechanical strength. Our studies have indicated that β-TCP scaffolds sintered to 1100°C for 12 h presented adequate mechanical and biological competence required to reestablish form and function at the host site.[3] While densification associated with ceramic heat treatment has been quantified, such parameters are typically dependent upon scaffold microgeometry, solid volume fraction, and nature of engineered porosities, among others, that can be controlled using CAD in the preprint stage.[43]

Leveraging Precision Control Over Pore Architecture with 3DP to Modulate Biomimetic β-TCP Scaffold Degradation Rate

Extracellular matrix formation, vascular in-growth, and nutrient/waste exchange depend on the geometric properties (pore architecture) of the scaffold.[37,42,44] Although solid (bulk) β-TCP constructs can be absorbed over time, the slow degradation rate limits its use in a growing skeleton where grafts are required to remodel with the patient.[49,67] Leveraging DIW 3D printing to manufacture resorbable β-TCP scaffolds using engineered pore architecture helps maximize construct rigidity with efficient vascular ingrowth, osteogenesis, and degradation kinetics.[45] As a proof of concept, 1-month-old (skeletally immature) New Zealand White rabbits (NZWR) underwent creation of unilateral 10 mm diameter calvarial defects.[45] Each defect received a β-TCP scaffold and monitored up to 18 months. When comparing the scaffold occupancy at different healing times (Fig. 4a), scaffolds showed significantly decreased presence *in vivo* (Fig. 4b).

To summarize, the study demonstrated an acceleration of β-TCP degradation to ∼55% a year owing to engineered pore architectures. Absorbed β-TCP was replaced by vascularized, organized bone with mechanical properties similar to native bone (Fig. 4c), demonstrating the efficacy of this particular tissue engineering method in BTR and justifying further preclinical translation.

Advancing Preclinical Translation Using Biomimetic β-TCP Scaffolds

Congenital craniomaxillofacial defects

One third of all congenital birth defects result in craniomaxillofacial congenital anomalies such as alveolar clefts.[68] Approximately three out of four cleft lip and palate patients present with an alveolar osseous defect resulting in facial asymmetry, insufficient osseous support, or nasal regurgitation. Other conditions may present themselves over the course of a patient's life, such as edentulism.[39] In some cases, autologous bone graft from the calvaria, iliac crest, and costal cartilage is limited by the volume and shape of harvestable bone, donor-site morbidity, and in some instances a risk of infection. Furthermore, unlike adult patients, the thickness of pediatric bone is thinner and could lead to a reduction in the osteoconductive potential of the autologous bone graft.[63] Moreover, considering long-term growth and development of the craniofacial skeleton, patients may experience growth restriction and require multiple revision surgeries.

The ideal pediatric bone replacement would therefore need to effectively fit and fill the defect site and restore structure and function while preserving harmonic growth without impeding facial development. However, autogenous bone grafting may not be sufficient in patients that have wider or bilateral clefts. Furthermore, as such defects may

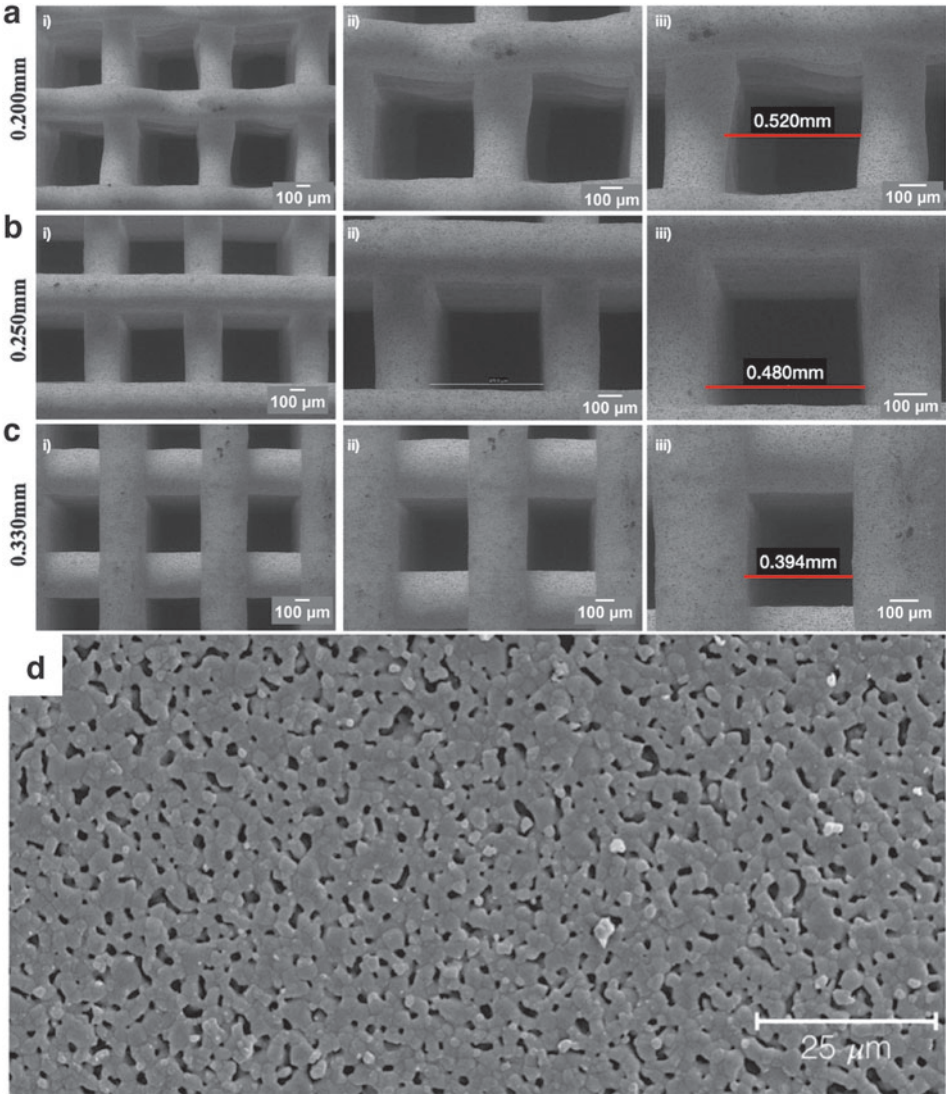

FIG. 3. Scanning electron microscope images of 3D printed β-TCP scaffolds printed with different nozzle diameters. **(a)** 0.200 mm, **(b)** 0.250 mm, **(c)** 0.330 mm. **(i, ii, iii)** Show capacity of DIW to fabricate scaffolds with varying pore sizes, and **(d)** microgeometry and surface texture of β-TCP scaffold sintered to 1100°C for 4 h.[3,46] β-TCP, β-tricalcium phosphate.

be critically sized, additional surgical intervention may be necessary. Due to these unique considerations, efficacious translation of bone tissue engineering strategies in a pediatric context has been limited.[69–72]

As an alternative treatment modality to autologous bone grafting, skeletally immature NZWR were used as a model for alveolar cleft regeneration using 3DP β-TCP scaffolds.[73] Unlike the random bone formation that would occur with the use of conventional granular grafts, new bone formation was observed both within the scaffold and at the interstices between osteotomy (3.5×3.5 mm) and construct (Fig. 5a). The newly formed bone was also highly cellular and vascularized.[73] Although this body of work provided foundational evidence of the effectiveness of biomimetic ceramic scaffolds in regenerating pediatric craniofacial defects, future human application warranted successful implementation in a large preclinical, translational animal model.

A recent study on healing critically sized calvarial defects (~ 1.4 cm diameter) using 3DP β-TCP scaffolds in a swine model revealed no adverse signs of healing (Fig. 5b). An intramembranous-like healing was observed with osteoconduction having occurred throughout all scaffold porous dimensions from defect margins toward the center of critical-sized defects.[74] Most importantly, bone conduction was greater in defects containing a scaffold, when compared to empty defects. While the efficacy in treating critically sized defects using 3DP scaffolds is promising, complex fractures arising from traumatic events present additional challenges. In particular, there is a need for mechanically robust 3DP scaffolds to effectively restore form and function at defect sites that are typically under physiological loading.

Noncongenital defects

Critically sized defects in the maxillofacial complex. Craniofacial trauma may impart large forces to the cranium and facial bones, resulting in large deficits of bone requiring reconstruction. Extensively sized repair sites in the mandible often require close approximation of the synthetic grafting material to the defect margins.[3,30,31,36,38,39,42,43,45,55,60,75–79] This is particularly difficult in the case of granular-based grafting materials as they cannot be properly shaped to fit and fill defects requiring extensive subsequent remodeling for complete repair.[80] This issue is exacerbated in load-bearing sites such as the mandible.

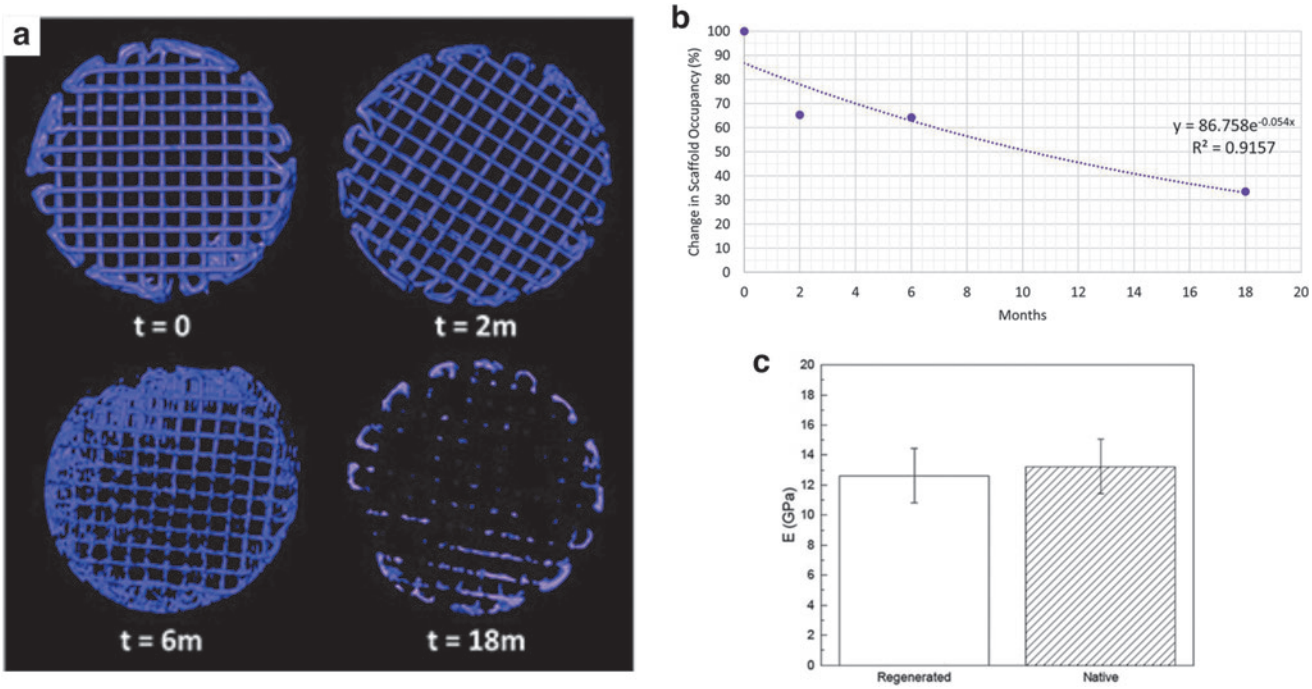

FIG. 4. **(a)** Three-dimensional reconstructions of scaffold (*purple*) in the calvarium (image not to scale), **(b)** degradation kinetics analysis of scaffold over 18 months used to calculate annual degradation rate of β-TCP in the calvarium, and **(c)** elastic modulus (E) of calvarial scaffold-regenerated bone shows no difference compared to that of native control. Error bars are 95% confidence intervals.[45]

In studies using 3DP β-TCP scaffolds in load-bearing applications (Fig. 6a, b), the regenerative capacity of bioceramic scaffolds have yielded favorable results. In one study, full-thickness, unilateral defects were induced in skeletally mature NZWR at the segmental mandibular body and filled with 3DP β-TCP scaffolds. Scaffolds demonstrated bone regeneration at 8 weeks *in vivo* (Fig. 6c).[38] Scaffolds were observed to bridge the span of the defect with intramembranous-like healing and vascularized woven bone formation in and around the scaffold. These results demonstrated the ability of 3DP β-TCP scaffolds to support BTR in the presence of physiological loading during masticatory function.

Critically sized defects in the lower extremities

At the onset of fracture healing, a weak osteogenic interface forms between newly forming and original bone, permitting bone remodeling through coupled osteoblastic and osteoclastic activity. This innate mechanism is often inadequate in settings

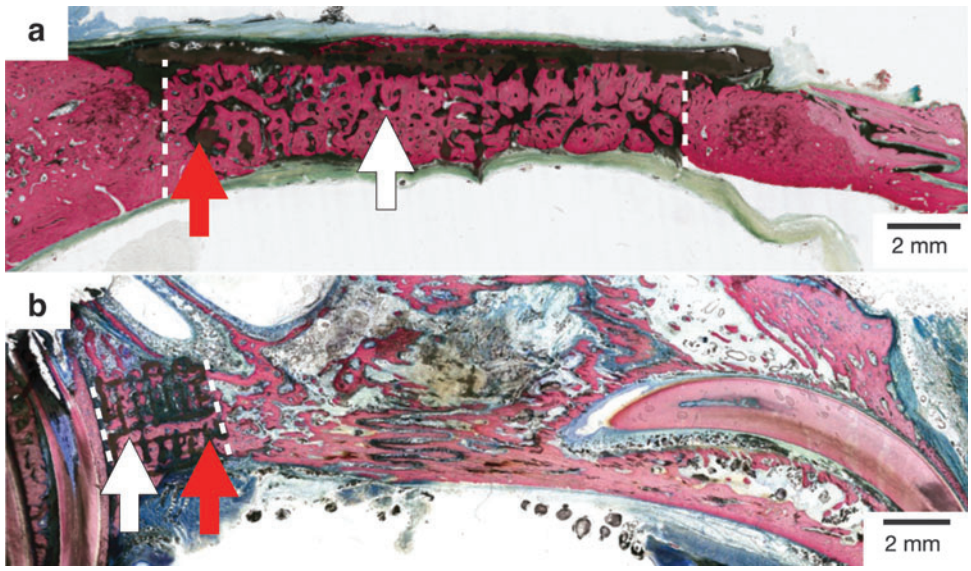

FIG. 5. Nondecalcified histologic sections of **(a)** calvarial defect and **(b)** alveolar defect filled with 3DP scaffolds. *Red arrows* indicate biomimetic ceramic scaffolds and *white arrows* indicate organized bone formation within the engineered pores of the scaffolds.[73,74] *White dashed lines* denote the ends/margins of the 3D printed scaffold. 3DP, three-dimensional printing.

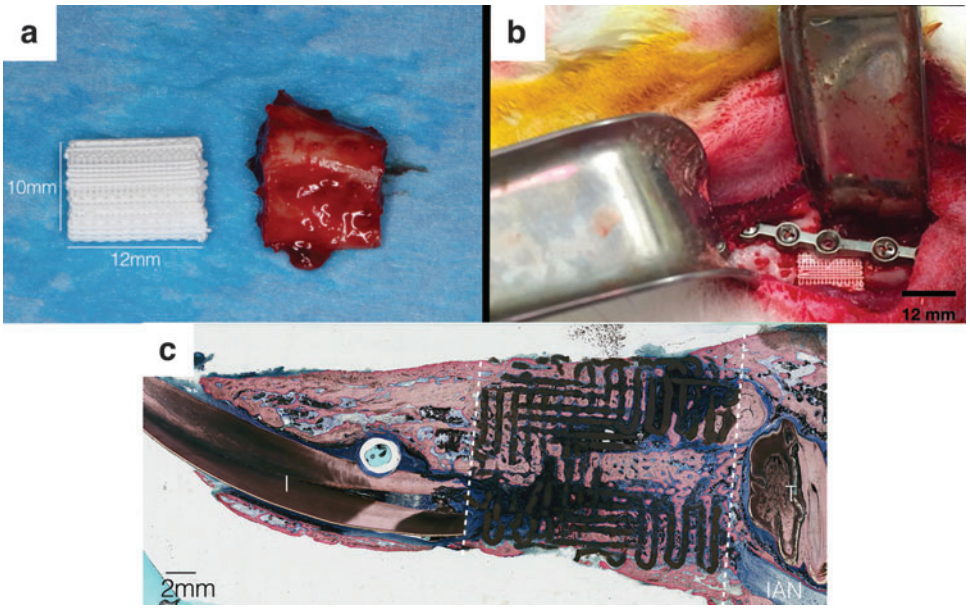

FIG. 6. **(a)** Surgical segment compared to scaffold **(b)** surgical placement of scaffold, and **(c)** sagittal histologic slice of scaffold in continuity with rabbit mandible. *White dashed lines* denote the ends/margins of the 3D printed scaffold. I, incisor; IAN, inferior alveolar nerve; T, tooth.[38]

that require significant boney and soft tissue regeneration such as in extensive lower extremity trauma.[3] Large defects present reconstructive challenges given the vast amounts of hard tissue that need to be replaced (Fig. 7a). The treatment of large lower extremity defects is hence fundamentally different when compared to treating lesions in the upper extremity, where one of the current solutions is tissue transfer from the contralateral side. While this technique can provide resurfacing of fat and skin, it can only provide small bony segments, not suitable for larger grafts required for long bones in the lower extremities.[43,81]

A study utilizing osteoconductive, 3DP β-TCP scaffolds reported promising results in the restoration of full thickness segmental defects ($\sim$11 mm length × full thickness) in the radial diaphysis in NZWR. Upon gross examination and histologically, no signs of pain or swelling were reported. In addition, a tissue interface was observed between the 3DPBC and the remodeling bone at all time points evaluated. Qualitative microCT data indicated directional bone ingrowth along the bone long axis, with an increase in bone formation toward the original bone morphology over

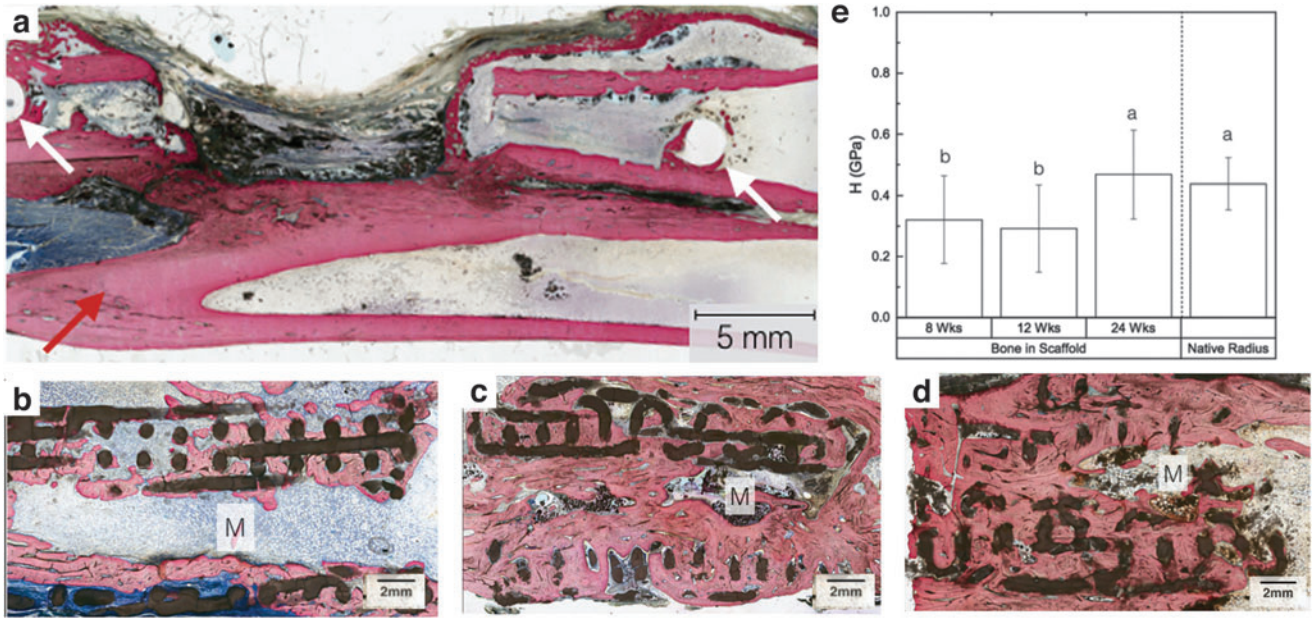

FIG. 7. Histological cross section of **(a)** negative control defect in the radius, with the *white arrows* indicating the screw locations for the surgical hardware; radius defect along the long axis of the 3D printed bioceramic scaffold at the defect site at **(b)** 8 weeks, **(c)** 12 weeks, and **(d)** 24 weeks. The marrow (M) space is visible with *yellow* marrow observed at 12- and 24-week time points, and **(e)** nanoindentation values of hydrated bone samples at 8, 12, and 24 weeks with native radius for comparison of hardness (H) of bone (The letters represent statistically homogeneous results). H at 8 and 12 weeks had similar means, whereas the values at 24 weeks were statistically >2 previous time points and achieved statistical homogeneity values relative to native bone.[3]

time. Resorption was seen as early as 8 weeks, with a substantially greater amount of bone regeneration of the radii marrow space at 12 and 24 weeks (Fig. 7b–d).

Osteoid formation and osteocytes were also found in close proximity with bioactive ceramic struts, with active remodeling of osteocytes, osteoblasts, and osteoclasts not only on the surface but also within the scaffold's engineered, biomimetic porous network. Furthermore at 24 weeks, the scaffold was observed to have significantly resorbed, presenting extensive structural discontinuity. Degradation was apparent as the original scaffold with a circular cross-section took on an increasingly discontinuous and irregularly shaped form, especially at 24 weeks.[43] More importantly, nanoindentation corroborated the histologic findings and reported the reestablishment of a bone network with histomorphology consistent with mature cortical-like native bone (Fig. 7e).[43]

In summary, static physical constructs printed using β-TCP colloidal gels exhibited the ability to support bone formation and enabled the restoration of form and function at the site of the induced defect, even in the presence of physiological loading. However, during surgical procedures, any correction/modification to cater toward a desired fit involves either resection of additional bone at the surgical site or, in the case of an oversized graft—abrasive instrument, to satisfy dimensional restrictions and/or constraints. While the former results in a fresh supply of cells toward the scaffold surface, the latter could compromise macro- and microlevel surface properties of the graft.

Most importantly, in cases where the critically sized defect site has an irregular shape, the nature of the ceramic grafts may not completely satisfy all dimensional requirements.[82] A 3D printed graft/scaffold that can cater to an irregularly shaped defect and be adjusted spontaneously through a stimulus would help solve some issues with static constructs.

Dynamic shape-memory bioceramic composite constructs

Research conducted on aliphatic polyesters (APs) such as polylactic acid (PLA) has enabled the development of a smart biodegradable subclass, termed shape-memory polymers (SMPs) which are quickly gaining interest in the biomedical industry.[83] Shape-memory effect (SME) of polymers is a fairly old concept described in 1953.[84] Since then, it has been studied in different polymers and polymer-composite systems.[85,86] These programmable materials have the capacity to ''memorize'' a geometrical configuration and be ''deformed'' to a temporary shape through polymer chain vitrification or crystallization. Furthermore, they can be reverted back to their original, memorized, permanent shape through external stimuli (i.e., heat).[83,87]

In the medical device industry, SMPs have thus far been utilized in minimally invasive surgery as well as for sutures.[85,86] SMPs are also being used in stents, however, their application has been limited, owing to the slow expansion characteristics postactuation. This has been previously reported to cause migration after insertion, which fortunately do not pose a major issue in the field of BTR where slow actuation can be accommodated.[88] In addition, unlike metal or metal alloys, APs do not cause stress shielding, further bolstering their suitability for BTR.[89] Perhaps more importantly, the shape-memory properties of APs and their osteogenic potential have been reported to improve after augmentation or combination with copolymers or inorganic particles such as β-TCP.[85,90]

Results from pilot studies incorporating β-TCP in a PLA matrix have indicated an enhancement in osteogenic potential of the overall composite construct and the ability to be mechanically actuated—to trigger transformative responses in the construct/material. Shape-memory structures manufactured through DIW were capable of expansion/contraction upon using heat as an external stimulus.

Molecular processes can help explain the underlying mechanisms of polymer chain mobility during these heating and cooling cycles. During changes in temperature, two separate domains of the system are theorized to play a pivotal role in SME, namely the crystalline domain or fixed parts (crystallized PLA chains), and amorphous or switching parts such as the long polymeric chains.[91] While the shape-fixing parts or net points are responsible for maintaining dimensional stability during deformation and recovery, shape-switching parts store elastic energy that enable SME.[91] In addition, glass transition temperature of a polymer (Tg)—the temperature at which polymer chains begin to move, also plays a vital role in SME actuation.[92] Below Tg, the polymer chains are stronger, and the constructs demonstrate higher stiffness and mechanical strength—like a solid.[93] Above Tg, polymer chains are free to move/flow and exhibit fluid-like behavior.[93] At Tg, constructs experience a transition from a rigid state to a more flexible state and demonstrate a behavior characterized as a ''rubbery'' phase.[93]

As a result, at this rubbery region, shape-memory materials exhibit large elongations/contractions under relatively low load that would facilitate SME actuation.[94–96] Perhaps more importantly from a clinical perspective, DIW 3DP constructs' shape-memory properties were unaltered after successive shape-memory cycles (Fig. 8a, b). This indicated the construct's ability to exhibit shape reconfiguration, giving surgeons the ability to further tailor the shape of constructs *in situ*, during surgical procedures, to effectively fit-and-fill irregularly shaped bone defect sites.

Future Perspectives and Challenges Using Bioactive, Biomimetic, 3D Printed Constructs

Recent translational studies have facilitated critical advancements in 3D-printed biomimetic scaffolds for boney defect repair in preparation for clinical utilization. Continued efforts should hence be directed toward long-term analysis of bone quality and effects of scaffold induced bone growth on skeletal maturity. In this regard, numerous strategies have been developed to optimize scaffold design. More recently, efforts have been directed toward utilizing growth factors to improve bone tissue repair.[36,43,73,75,78–80,97,98] Bone morphogenic protein (BMP) is one such osseoinductive protein that stimulates osteoblast proliferation and differentiation.[29,99] Specifically, BMP-2 is FDA-approved for maxillary sinus augmentation and noncritical alveolar ridge defects.[98,99] However, the treatment of defects with BMPs has been shown to cause ectopic bone formation and premature suture fusion (Fig. 9a).[100–102] In addition, while they act locally to induce the differentiation of

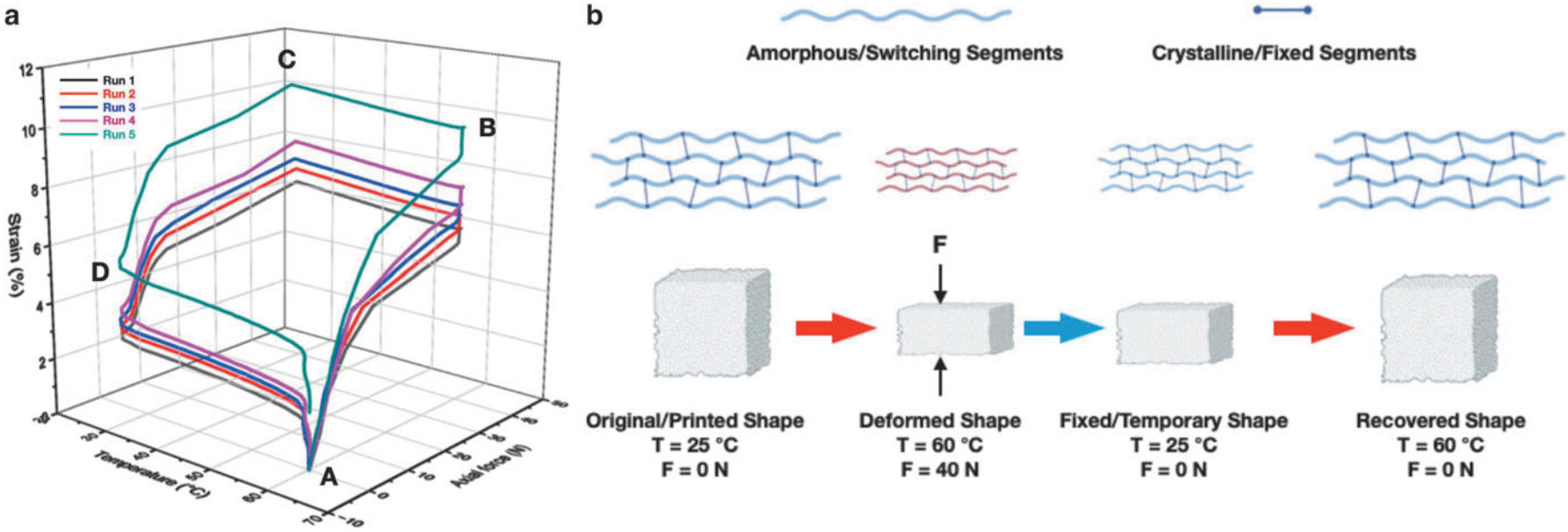

FIG. 8. **(a)** Stacked plot of repetitive shape-memory cycles indicating successive shape transformations through five different shape-memory cycles. Induced strains alter the shape of the construct—the shape is ''frozen in'' if it is maintained constant while temperature is decreased below Tg (B–C), and ''recovered'' if it is once again heated above Tg (D–A), and **(b)** illustration of the 1-W SME process. SME, shape-memory effect. Image generated on Biorender.com

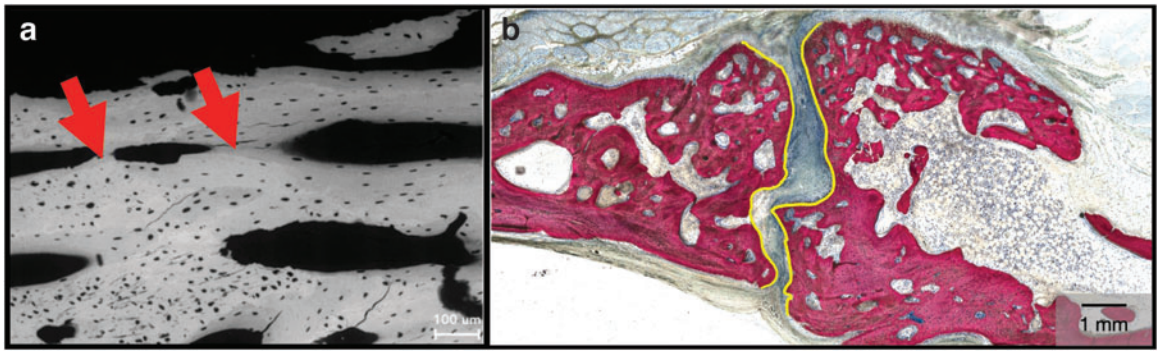

FIG. 9. **(a)** SEM micrograph of scaffold augmented with rhBMP-2 with signs of suture fusion (*red arrows*),[73] and **(b)** nondecalcified histology of calvarial scaffold shows blood vessels stained with Stevenel's *blue* and patent sutures with evidence of suture patency (*yellow* splines) adjacent to sites of reconstruction.[45] rhBMP-2, recombinant human bone morphogenetic protein-2.

mesenchymal stem cells into bone and cartilage cells, rapid local clearance is known to be a potential drawback.[103]

Consequently, alternative approaches to adenosine receptor activation, such as pharmacological manipulation, have been explored. Of note, Dipyridamole (DIPY), an adenosine A_{2A} receptor indirect agonist blocks adenosine reuptake into the cell via type 1 equilibrative nucleoside transporter, ENT1, thereby resulting in extracellular adenosine accumulation.[36,43,60,73–75,104–106] Studies utilizing 3DP β-TCP scaffolds have indicated improvements in bone regenerative capacities in the presence of DIPY in preclinical animal models.[36,43,60,73,75] 3D printed ceramic scaffolds augmented with DIPY have been shown to facilitate localized drug delivery to the defect site and to promote bone regeneration without disruption of suture patency (Fig. 9b).[73] Despite the strengths of these studies, several limitations exist that warrant further research. For example, smaller animal models may not accurately simulate all the anatomical complexities of the human craniofacial region (e.g., size, volume, interface of different tissues).[73]

Although studies have indicated efficacy of biomimetic, and bioactive scaffolds to rapidly regenerate bony defects using tissue engineering principles, this has yet to be realized in extensive long-term studies through preclinical translation in large animal models allowing researchers to evaluate the regenerative capacity of bioactive ceramic scaffolds more comprehensively.

Furthermore, while the clinical repair of hard tissues is constantly evolving based on emerging technology and new surgical techniques, research efforts must be directed toward standardizing protocols for the design, fabrication, and evaluation of 3D printed medical devices. Specifically, quality control measures and performance criteria must be thoroughly established. In addition, optimizing process parameters, strengthening market supervision, and addressing regulatory concerns can further promote the development of 3D printed tissue engineering scaffolds and ensure ease of accessibility to safe and efficacious treatment. Nevertheless, while new materials are being explored in a preclinical setting, research on biomimetic scaffolds for tissue engineering will continue to gain popularity among surgeons and translational researchers alike since it is amenable to a patient-specific approach.

Acknowledgment

The Zeiss Gemini 300 FE-SEM was provided courtesy of the National Institutes of Health S10 Shared Instrumentation Program (1A10OD026989-01).

Authors' Contributions

All authors have contributed equally to the drafting, writing, and editing of this invited review.

Disclosure Statement

No competing financial interests exist.

Funding Information

Some of the work referenced/discussed in this review was supported by DoD (W81XWH-16-1-0772 MPI-Rodriguez); NIH-NIAMS (R01AR068593—MPI: Paulo G. Coelho and Bruce N. Cronstein); NIH-NICHD (R21HD090664—MPI: Paulo G. Coelho, Bruce N. Cronstein, and Roberto L. Flores; R33HD090664—MPI: Paulo G. Coelho, Bruce N. Cronstein, Roberto L. Flores, and Lukasz Witek) and the Osteo Science Foundation (Peter Geistlich Research Award—MPI: Simon Young, F. Kurtis Kasper, Paulo G. Coelho, and Lukasz Witek).

References

1. Lanza RP. Principles of Tissue Engineering, 5th ed: Academic Press: London; 2020.
2. Seper L, Piffkó J, Joos U, et al. Treatment of fractures of the atrophic mandible in the elderly. J Am Geriatr Soc 2004;52(9):1583–1584.
3. Tovar N, Witek L, Atria P, et al. Form and functional repair of long bone using 3D printed bioactive scaffolds. J Tissue Eng Regen Med 2018;12(9):1986–1999.
4. Bernardo MP, da Silva BCR, Hamouda AEI, et al. PLA/hydroxyapatite scaffolds exhibit in vitro immunological inertness and promote robust osteogenic differentiation of human mesenchymal stem cells without osteogenic stimuli. Sci Rep 2022;12(1):2333.
5. Kenley RA, Yim K, Abrams J, et al. Biotechnology and bone graft substitutes. Pharm Res 1993;10(10):1393–1401.

6. Steijvers E, Ghei A, Xia Z. Manufacturing artificial bone allografts: A perspective. Biomater Transl 2022; 3(1):65–80.
7. Qi L, Liu Y, Li H, et al. Results of 10-year follow-up of the iliac donor site of graft patients. J Int Med Res 2014;42(6):1348–1352.
8. Matsuura T, Hashimoto Y, Kinoshita T, et al. Donor site evaluation after osteochondral autograft transplantation for capitellar osteochondritis dissecans. Am J Sports Med 2019;47(12):2836–2843.
9. Fukuba S, Okada M, Nohara K, et al. Alloplastic bone substitutes for periodontal and bone regeneration in dentistry: Current status and prospects. Materials (Basel) 2021;14(5):1096.
10. Rodriguez Colon R, Nayak VV, Parente PE, et al. The presence of 3D printing in orthopedics: A clinical and material review. J Orthop Res 2023;41(3):601–613.
11. Dawood A, Marti BM, Sauret-Jackson V, et al. 3D printing in dentistry. Br Dent J 2015;219(11):521.
12. Trautz OR, Legeros RZ, Legeros J. Effect of magnesium on various calcium phosphates. J Dent Res 1964;43:17.
13. Koeneman J, Lemons J, Ducheyne P, et al. Workshop on characterization of calcium phosphate materials. J Appl Biomater 1990;1(1):79–90.
14. Ducheyne P, Hench L, Kagan A, et al. Effect of hydroxyapatite impregnation on skeletal bonding of porous coated implants. J Biomed Mater Res 1980;14:225–237.
15. Ducheyne P, De Groot K. In vivo surface activity of a hydroxyapatite alveolar bone substitute. J Biomed Mater Res 1981;15(3):441–445.
16. Ducheyne P, Van Raemdonck W, Heughebaert J, et al. Structural analysis of HA coating on titanium. Biomaterials 1986;7:97–103.
17. Ducheyne P. Titanium and calcium phosphate ceramic dental implants, surfaces, coatings and interfaces. J Oral Implantol 1988;14:325–340.
18. Ducheyne P, Beight J, Cuckler J, et al. Effect of calcium phosphate coating characteristics on early post-operative bone tissue ingrowth. Biomaterials 1990;11:531–540.
19. Baker M, Eberhardt A, Martin D, et al. Bone properties surrounding hydroxyapatite-coated custom osseous integrated dental implants. J Biomed Mater Res B Appl Biomater 2010;95:218–224.
20. Zafar MJ, Zhu D, Zhang Z. 3D printing of bioceramics for bone tissue engineering. Materials (Basel) 2019;12(20): 3361.
21. Ly M, Spinelli S, Hays S, et al. 3D printing of ceramic biomaterials. Eng Regen 2022;3(1):41–52.
22. Du X, Fu S, Zhu Y. 3D printing of ceramic-based scaffolds for bone tissue engineering: An overview. J Mater Chem B 2018;6(27):4397–4412.
23. Bose S, Roy M, Bandyopadhyay A. Recent advances in bone tissue engineering scaffolds. Trends Biotechnol 2012;30(10):546–554.
24. Li Z, Li Z, Xu R, et al. Three-dimensional printing models improve understanding of spinal fracture—A randomized controlled study in China. Sci Rep 2015;5:11570.
25. Rengier F, Mehndiratta A, von Tengg-Kobligk H, et al. 3D printing based on imaging data: review of medical applications. Int J Comput Assist Radiol Surg 2010;5(4): 335–341.
26. Ma L, Zhou Y, Zhu Y, et al. 3D printed personalized titanium plates improve clinical outcome in microwave ablation of bone tumors around the knee. Sci Rep 2017;7(1):7626.
27. Dipaola M, Wodajo FM. 3D Printing in Orthopaedic Surgery. Elsevier: St. Louis, MO; 2019.
28. Gungor-Ozkerim PS, Inci I, Zhang YS, et al. Bioinks for 3D bioprinting: An overview. Biomater Sci 2018;6(5):915–946.
29. Aghaloo TL, Hadaya D. Basic principles of bioengineering and regeneration. Oral Maxillofac Surg Clin 2017; 29(1):1–7.
30. Wu V, Helder MN, Bravenboer N, Ten Bruggenkate CM, et al. Bone tissue regeneration in the oral and maxillofacial region: A review on the application of stem cells and new strategies to improve vascularization. Stem Cells Int 2019;2019:6279721.
31. Hollinger JO, Kleinschmidt JC. The critical size defect as an experimental model to test bone repair materials. J Craniofac Surg 1990;1(1):60–68.
32. Reychler H, Iriarte Ortabe J, Pecheur A, et al. Mandibular reconstruction with a free vascularized fibula flap and osseointegrated implants: A report of four cases. J Oral Maxillofac Surg 1996;54(12):1464–1469.
33. Shaw RJ, Sutton AF, Cawood JI, et al. Oral rehabilitation after treatment for head and neck malignancy. Head Neck 2005;27(6):459–470.
34. Hoffman HT, Harrison N, Sullivan MJ, et al. Mandible reconstruction with vascularized bone grafts. A histologic evaluation. Arch Otolaryngol Head Neck Surg 1991; 117(8):917–925.
35. Twohig C, Helsinga M, Mansoorifar A, et al. A dual-ink 3D printing strategy to engineer pre-vascularized bone scaffolds in-vitro. Mater Sci Eng C Mater Biol Appl 2021;123:111976.
36. Lopez CD, Diaz-Siso JR, Witek L, et al. Dipyridamole augments three-dimensionally printed bioactive ceramic scaffolds to regenerate craniofacial bone. Plast Reconstr Surg 2019;143(5):1408–1419.
37. Maroulakos M, Kamperos G, Tayebi L, et al. Applications of 3D printing on craniofacial bone repair: A systematic review. J Dent 2019;80:1–14.
38. Lopez CD, Diaz-Siso JR, Witek L, et al. Three dimensionally printed bioactive ceramic scaffold osseoconduction across critical-sized mandibular defects. J Surg Res 2018;223:115–122.
39. Witek L, Colon RR, Wang MM, et al. Tissue-engineered alloplastic scaffolds for reconstruction of alveolar defects. Handb Tissue Eng Scaffolds 2019;1:505–520.
40. Bauermeister AJ, Zuriarrain A, Newman MI. Three-dimensional printing in plastic and reconstructive surgery: A systematic review. Ann Plast Surg 2016;77(5):569–576.
41. Witek L, Nayak VV, Runyan CM, et al. Tissue Engineering Strategies for Craniomaxillofacial Surgery: Current Trends in 3D-Printed Bioactive Ceramic Scaffolds. In: Innovative Bioceramics in Translational Medicine II: Surgical Applications. (Choi AH, Ben-Nissan B. eds.) Springer Singapore: Singapore; 2022; pp. 55–74.
42. Zhang Z. Bone regeneration by stem cell and tissue engineering in oral and maxillofacial region. Front Med 2011;5(4):401–413.
43. Witek L, Alifarag AM, Tovar N, et al. Repair of critical-sized long bone defects using dipyridamole-augmented 3D-printed bioactive ceramic scaffolds. J Orthop Res 2019;37(12):2499–2507.
44. Kinoshita Y, Maeda H. Recent developments of functional scaffolds for craniomaxillofacial bone tissue engineering applications. ScientificWorldJournal 2013;2013:863157.

45. Shen C, Wang MM, Witek L, et al. Transforming the degradation rate of β-tricalcium phosphate bone replacement using 3-dimensional printing. Ann Plast Surg 2021; 87(6):e153–e162.
46. Arbex L, Nayak VV, Ricci JL, et al. Physio-mechanical and biological effects due to surface area modifications of 3D printed β-tri-calcium phosphate: An in vitro study. Ann 3D Print Med 2022;8:100078.
47. Lopez CD, Witek L, Flores RL, et al. 3D Printing and Adenosine Receptor Activation for Craniomaxillofacial Regeneration. In: Regenerative Strategies for Maxillary and Mandibular Reconstruction: A Practical Guide. (Melville JC, Shum JW, Young S, Wong ME. eds.) Springer International Publishing: Cham; 2019; pp. 255–267.
48. Brown PW. Calcium Phosphates in Biomedical Engineering. In: Encyclopedia of Materials: Science and Technology. (Buschow KHJ, Cahn RW, Flemings MC, et al. eds.) Elsevier: Oxford; 2001; pp. 893–897.
49. Moore WR, Graves SE, Bain GI. Synthetic bone graft substitutes. ANZ J Surg 2001;71(6):354–361.
50. Hench LL. Bioceramics. J Am Ceram Soc 1998;81(7): 1705–1728.
51. Hench LL. Bioceramics: From concept to clinic. J Am Ceram Soc 1991;74(7):1487–1510.
52. Babis GC, Soucacos PN. Bone scaffolds: The role of mechanical stability and instrumentation. Injury 2005; 36(4 Suppl):S38–S44.
53. Truumees E, Herkowitz HN. Alternatives to autologous bone harvest in spine surgery. Univ Pennsylvania Orthop J 1999;12:77–88.
54. Coelho PG, Eckstein D, Rivera C, et al. Physical and chemical characterization of synthetic bone mineral ink—For additive manufacturing applications. Ann 3D Print Med 2021;3:100024.
55. Shen C, Witek L, Flores RL, et al. Three-dimensional printing for craniofacial bone tissue engineering. Tissue Eng Part A 2020;26(23–24):1303–1311.
56. Lu H, Zhou Y, Ma Y, et al. Current application of beta-tricalcium phosphate in bone repair and its mechanism to regulate osteogenesis. Front Mater 2021;8:698915.
57. Kang H-J, Makkar P, Padalhin AR, et al. Comparative study on biodegradation and biocompatibility of multichannel calcium phosphate based bone substitutes. Mater Sci Eng C 2020;110:110694.
58. Gilev M, Bazarny V, Volokitina E, et al. Laboratory monitoring of bone tissue remodeling after augmentation of impression intraarticular fracture with different types of bone graft. Bull Exp Biol Med 2019;167:681–684.
59. Pereira R, Gorla L, Boos F, et al. Use of autogenous bone and beta-tricalcium phosphate in maxillary sinus lifting: histomorphometric study and immunohistochemical assessment of RUNX2 and VEGF. Int J Oral Maxillofac Surg 2017;46(4):503–510.
60. Lopez CD, Witek L, Torroni A, et al. The role of 3D printing in treating craniomaxillofacial congenital anomalies. Birth Defects Res 2018;110(13):1055–1064.
61. Witek L. Extrusion-Based, Three-Dimensional Printing of Calcium-Phosphate Scaffolds. Oklahoma State University: Stillwater, OK; 2015.
62. Sweet L, Kang Y, Czisch C, et al. Geometrical versus random β-TCP scaffolds: Exploring the effects on Schwann cell growth and behavior. PLoS One 2015;10(10):e0139820.
63. Wang MM, Flores RL, Witek L, et al. Dipyridamole-loaded 3D-printed bioceramic scaffolds stimulate pediatric bone regeneration in vivo without disruption of craniofacial growth through facial maturity. Sci Rep 2019;9(1):18439.
64. Flores RL, Liss H, Raffaelli S, et al. The technique for 3D printing patient-specific models for auricular reconstruction. J Craniomaxillofac Surg 2017;45(6):937–943.
65. Witek L, Khouri KS, Coelho PG, et al. Patient-specific 3D models for autogenous ear reconstruction. Plast Reconstr Surg Glob Open 2016;4(10):e1093.
66. Silva NR, Witek L, Coelho PG, et al. Additive CAD/CAM process for dental prostheses. J Prosthodont 2011;20(2): 93–96.
67. Kivrak N, Taş AC. Synthesis of calcium hydroxyapatite-tricalcium phosphate (HA-TCP) composite bioceramic powders and their sintering behavior. J Am Ceram Soc 1998;81(9):2245–2252.
68. Gorlin RJ, Cohen MM, Jr. Hennekam RC. Syndromes of the Head and Neck. Oxford University Press: New York, NY; 2001.
69. Caballero M, Jones DC, Shan Z, et al. Tissue engineering strategies to improve osteogenesis in the juvenile swine alveolar cleft model. Tissue Eng Part C Methods 2017; 23(12):889–899.
70. Smartt JM, Jr. Karmacharya J, Gannon FH, et al. Repair of the immature and mature craniofacial skeleton with a carbonated calcium phosphate cement: Assessment of biocompatibility, osteoconductivity, and remodeling capacity. Plast Reconstr Surg 2005;115(6):1642–1650.
71. Patel M, Fisher JP. Biomaterial scaffolds in pediatric tissue engineering. Pediatr Res 2008;63(5):497–501.
72. Tevlin R, McArdle A, Atashroo D, et al. Biomaterials for craniofacial bone engineering. J Dent Res 2014;93(12): 1187–1195.
73. Lopez CD, Coelho PG, Witek L, et al. Regeneration of a pediatric alveolar cleft model using three-dimensionally printed bioceramic scaffolds and osteogenic agents: comparison of dipyridamole and rhBMP-2. Plast Reconstr Surg 2019;144(2):358–370.
74. DeMitchell-Rodriguez EM, Shen C, Nayak VV, et al. Bone tissue engineering in the growing calvaria: A 3D printed bioceramic scaffold to reconstruct critical-sized defects in a skeletally immature pig model. Plast Reconstr Surg 2023:10.1097.
75. Bekisz JM, Flores RL, Witek L, et al. Dipyridamole enhances osteogenesis of three-dimensionally printed bioactive ceramic scaffolds in calvarial defects. J Craniomaxillofac Surg 2018;46(2):237–244.
76. Fama C, Kaye GJ, Flores R, et al. Three-dimensionally-printed bioactive ceramic scaffolds: Construct effects on bone regeneration. J Craniofac Surg 2021;32(3):1177–1181.
77. Melville JC, Manon VA, Blackburn C, et al. Current methods of maxillofacial tissue engineering. Oral Maxillofac Surg Clin North Am 2019;31(4):579–591.
78. Schliephake H. Clinical efficacy of growth factors to enhance tissue repair in oral and maxillofacial reconstruction: A systematic review. Clin Implant Dent Relat Res 2015;17(2):247–273.
79. Talaat WM, Ghoneim MM, Salah O, et al. Autologous bone marrow concentrates and concentrated growth factors accelerate bone regeneration after enucleation of mandibular pathologic lesions. J Craniofac Surg 2018; 29(4):992–997.
80. Helenius LM, Hallikainen D, Helenius I, et al. Clinical and radiographic findings of the temporomandibular joint

in patients with various rheumatic diseases. A case-control study. Oral Surg Oral Med Oral Pathol Oral Radiol Endod 2005;99(4):455–463.
81. Reigstad A, Hetland K, Bye K, et al. Free flaps in the reconstruction of hand and distal forearm injuries. J Hand Surg 1992;17(2):185–188.
82. Wang F, Yuan C, Wang D, et al. A phase evolution based constitutive model for shape memory polymer and its application in 4D printing. Smart Mater Struct 2020;29(5): 055016.
83. Subash A, Kandasubramanian B. 4D printing of shape memory polymers. Eur Polym J 2020;134:109771.
84. Flory PJ. Principles of Polymer Chemistry: Cornell University Press: Ithica, NY; 1953.
85. Senatov FS, Niaza KV, Zadorozhnyy MY, et al. Mechanical properties and shape memory effect of 3D-printed PLA-based porous scaffolds. J Mech Behav Biomed Mater 2016;57:139–148.
86. Neffe AT, Hanh BD, Steuer S, et al. Polymer networks combining controlled drug release, biodegradation, and shape memory capability. Adv Mater 2009;21(32–33): 3394–3398.
87. Bayart M, Charlon S, Soulestin J. Fused filament fabrication of scaffolds for tissue engineering; how realistic is shape-memory? A review. Polymer 2021;217:123440.
88. Senatov F, Zadorozhnyy MY, Niaza K, et al. Shape memory effect in 3D-printed scaffolds for self-fitting implants. Eur Polym J 2017;93:222–231.
89. Tseng L-F, Mather PT, Henderson JH. Shape-memory-actuated change in scaffold fiber alignment directs stem cell morphology. Acta Biomater 2013;9(11):8790–8801.
90. Lendlein A, Langer R. Biodegradable, elastic shape-memory polymers for potential biomedical applications. Science 2002;296(5573):1673–1676.
91. Mehrpouya M, Vahabi H, Janbaz S, et al. 4D printing of shape memory polylactic acid (PLA). Polymer 2021;230: 124080.
92. Hiltz JA. Shape Memory Polymers-Literature Review. Defence R&D Canada: Ottawa, ON; 2002.
93. Gu S, Yan B, Liu L, et al. Carbon nanotube–polyurethane shape memory nanocomposites with low trigger temperature. Eur Polym J 2013;49(12):3867–3877.
94. Tobushi H, Hara H, Yamada E, et al. Thermomechanical properties in a thin film of shape memory polymer of polyurethane series. Smart Mater Struct 1996;5(4):483.
95. Tobushi H, Ikai A, Yamada S, et al. Thermomechanical properties of TiNi shape memory alloy. J Phys IV 1996; 6(C1):C1-385–C1-393.
96. Quay J, Well JB, Lee C, et al. Prediction of polyurethane hard segment structures based on diphenylmethane-urethane model compounds. J Macromol Sci Part B 1985; 24(1–4):61–85.
97. Melville JC, Nassari NN, Hanna IA, et al. Immediate transoral allogeneic bone grafting for large mandibular defects. less morbidity, more bone. A paradigm in benign tumor mandibular reconstruction? J Oral Maxillofac Surg 2017;75(4):828–838.
98. Ramly EP, Alfonso AR, Kantar RS, et al. Safety and efficacy of recombinant human bone morphogenetic protein-2 (rhBMP-2) in craniofacial surgery. Plast Reconstr Surg Glob Open 2019;7(8):e2347.
99. Gomes-Ferreira PHS, Okamoto R, Ferreira S, et al. Scientific evidence on the use of recombinant human bone morphogenetic protein-2 (rhBMP-2) in oral and maxillofacial surgery. Oral Maxillofac Surg 2016;20(3):223–232.
100. Kinsella CR, Jr., Cray JJ, Durham EL, et al. Recombinant human bone morphogenetic protein-2-induced craniosynostosis and growth restriction in the immature skeleton. Plast Reconstr Surg 2011;127(3):1173–1181.
101. Shah RK, Moncayo VM, Smitson RD, et al. Recombinant human bone morphogenetic protein 2-induced heterotopic ossification of the retroperitoneum, psoas muscle, pelvis and abdominal wall following lumbar spinal fusion. Skeletal Radiol 2010;39(5):501–504.
102. Oetgen ME, Richards BS. Complications associated with the use of bone morphogenetic protein in pediatric patients. J Pediatr Orthop 2010;30(2):192–198.
103. Khojasteh A, Behnia H, Naghdi N, et al. Effects of different growth factors and carriers on bone regeneration: A systematic review. Oral Surg Oral Med Oral Pathol Oral Radiol 2013;116(6):e405–e423.
104. FitzGerald GA. Dipyridamole. N Engl J Med 1987; 316(20):1247–1257.
105. Patrono C, Coller B, Dalen JE, et al. Platelet-active drugs: the relationships among dose, effectiveness, and side effects. Chest 1998;114(5 Suppl):470S–488S.
106. Monagle P, Chan AKCKC, Goldenberg NA, et al. Antithrombotic therapy in neonates and children: Antithrombotic Therapy and Prevention of Thrombosis, 9th ed: American College of Chest Physicians Evidence-Based Clinical Practice Guidelines. Chest 2012;141(2 Suppl): e737S–e801S.

Address correspondence to:
Lukasz Witek, MSci, PhD
Biomaterials Division
New York University College of Dentistry
345 East 24th Street
Room 902D
New York, NY 10010
USA

E-mail: lukasz.witek@nyu.edu

Received: April 18, 2023
Accepted: June 20, 2023
Online Publication Date: July 18, 2023